Nigerian Journal of Mathematics and Applications
Volume **26**, (2017), 173 − 190. *Printed by Unilorin press*
©*Nig. J. Math. Appl.* *http://www.njmaman.com*

MHD Mixed Convective Flow of a Second Grade Fluid in the Presence of Nonlinearized Thermal Radiation, Thermal diffusion and Diffusion thermo Effects

I. G. Baoku [1*] and K. I. Falade[2]

Abstract

The implicit finite difference method of Crank-Nicolson type is employed to examine heat and mass transfer in a transient magnetohydrodynamic mixed convective flow of a viscoelastic second grade fluid past a vertical porous plate in the presence of nonlinearized thermal radiation, thermal diffusion and diffusion thermo effects. The governing coupled nonlinear time-based partial differential equations are non-dimensionalized by using appropriate dimensionless variables to obtain the dimensionless highly nonlinear partial differential forms of momentum, energy and species concentration equations. These equations are solved numerically in the presence of buoyancy force. The influences of different emerging parameters such as the suction parameter, second grade parameter, Prandtl number, Lewis number, thermal radiation parameter, temperature difference parameter, Dufour number, Soret number, mixed convection parameter and concentration buoyancy parameter on velocity, temperature and species concentration profiles are plotted and discussed.

Received: 27/10/2017, Accepted: 10/11/2017, Revised: 19/12/2017.
2015 *Mathematics Subject Classification.* 76Rxx & 37E35.
[*] Corresponding author.
Key words and phrases. MHD; Mixed Convection; Second Grade; Nonlinear Thermal Radiation; Thermal Diffusion; Diffusion thermo.
[1]Department of Mathematical Sciences, Federal University, Dutsin-Ma, P.M.B. 5001, Dutsin-Ma, Katsina State, Nigeria: E-mail: ibaoku@fudutsinma.edu.ng
[2]Department of Mathematics, Kano University of Science and Technology, P.M.B. 3244, Wudil, Kano State, Nigeria.

1. Introduction

The study of non-Newtonian fluids has gained the attention of many researchers because non-Newtonian fluids play significant roles in many industrial and technological applications. Few examples of non-Newtonian fluids are polymer solutions, foodstuffs, synthetic fibres, waste fluids and extrusion of molten plastics, etc. Modelling of viscoelastic non-Newtonian fluid flows is crucial for understanding and predicting the behaviour of processes. This aids the designing of optimal flow configuration and selecting several operating conditions. Governing equations of non-Newtonian fluids are of higher order than the Navier-Stoke's equations. A subclass of viscoelastic non-Newtonian fluids is the second grade fluid. The flow, heat and/or mass transfer of second grade fluid have been studied by Soundalgekar (1974), Rajagopal *et. al.* (1984), Dandapat and Gupta (1989), Bandelli and Rajagopal (1995), Nataraja *et. al.* (1998), Bhattacharyya *et. al.* (1998), Prasad *et. al.* (2001), Subhas and Veena. (1998), Ariel (2002), Vajravelu and Rollins (2004), Massoudi and Maneschy (2004), Siddheshwar and Mahabaleshwar (2005), Cortell (2006), Hayat *et. al.* (2008), Baoku *et. al.* (2015) with diverse problems under different configurations or geometries.

The survey of literature reveals that exhaustive information is available for steady flow, heat and mass transfer of second grade fluid from aforementioned researches and references therein. Some attempts have been made on the unsteady flow of second grade flow. The problem of unsteady boundary layer flow of a second grade over a stretching sheet for two heating processes namely the prescribed surface temperature (PST case) and prescribed surface heat flux (PHF case) was investigated Sajid *et. al.* (2009). They noted that the present solutions of a second grade were valid for all dimensionless times. The effects of an oscillatory motion of a viscoelastic fluid over infinite stretching sheet in porous media have been studied by Prasad *et. al.* (2000). They found that the velocity of the viscoelastic fluid decreased in the presence of porous media, as compared to the viscous fluid. The velocity profile and pressure gradient of the unsteady state unidirectional flow of second grade fluids between the parallel plates in which the flow motion in the plates was induced by a given arbitrary inlet volume flow rate which varied with time were considered by Chen *et. al.* (2003). The magnetohydrodynamic flow due to non-coaxial rotations of a porous disk, moving with uniform acceleration in its own plane and a second grade fluid at infinity was examined by Asghar *et. al.* (2007). They provided both analytically and numerically solutions to show effects of non-Newtonian fluid characteristics and uniform acceleration of the disk on the velocity field. The laminar flow problem of convective heat transfer for a second grade fluid over a semi-infinite plate in the presence of species concentration and chemical reaction was investigated Hayat *et. al.* (2008).

Fluid solid mixtures were considered as second grade fluids and are modeled as fluids with variable physical parameters by Asghar *et. al.* (2009). They used an eigen function expansion method to find the velocity distribution. Ali and Awais (2014) have used the numerical inversion of Laplace transform to study the time-dependent thin film flow of a second grade fluid flowing down an inclined plane through a porous medium. Khan *et. al.* (2017) have presented a Caputo-Fabrizio fractional derivatives approach to the thermal analysis of a second grade fluid over an infinite oscillating vertical flat plate. They obtained closed form solutions of the fluid velocity and temperature by means of the Laplace transform. They found that fractional fluids (second grade and Newtonian) have highest velocities and showed that the fractional parameter enhanced the fluid flow. Raza (2017) investigated some starting solutions corresponding to unsteady rotational flow of a second grade fluid with the non-integer Caputo-time fractional derivatives through an infinite long cylinder. They employed the inverse Laplace transformation, calculated numerically by using Stehfest's algorithm and showed that the hybrid technique presented has less computational effort and time cost as compared to other schemes in literature.

According to Fourier's and Fick's laws, some researchers neglected the thermal diffusion and diffusion thermo effects on heat and mass transfer on the basis that they are of a smaller order of magnitude. However, there are other exceptions especially when density differences exist in the flow regime. Eckert and Drake (1972) investigated several cases when the Dufour effect cannot be neglected. Afify (2009) expatiated that when heat and mass transfer occurred in a moving fluid, the mass fluxes can be developed by the temperature gradient, which is called thermal diffusion or Soret effect and that the energy flux can be generated by a composition gradient called the diffusion thermo or Dufour effect. He employed the similarity solution to study the MHD effect of thermal diffusion and diffusion thermo on a natural convective heat and mass transfer in the pressure of suction or injection over stretching surfaces. Hamad *et. al.* (2012) examined the effects of hydrodynamic slip and thermal convective boundary conditions on heat and mass with variable diffusivity using Lie group analysis. Thus, thermal diffusion and diffusion thermo effects have been found to appreciably influence the flow field in the heat and mass transfer phenomena.

Moreover, considerable interest has been shown in radiation interaction with convection for heat in fluid flow. This springs from the fact that thermal radiation in the surface heat transfer plays significant roles when a small convective heat transfer is considered, particularly in convective problems relating to absorbing-emitting fluids. Among the researchers who verified effects of thermal radiation on transport phenomena of fluids with optically thick or thin media are Makinde and Mhone (2005), Raptis and Perdikis (1999), Abel *et. al.* (2005), Siddheshwar and Mahabaleshwar (2005), Cortell (2007), Makinde (2005), Olanrewaju (2010),

Baoku *et. al.* (2012), Olajuwon and Baoku (2014), Popoola *et. al.* (2016) and Nabil *et. al.* (2017). In the aforementioned literature on thermal radiation effects, the linearized form of model for radiative heat flux has been used for optically thick media. However, the nonlinearized form of radiative heat flux depicts the actual heat emission or conduction in the energy characteristics of most boundary layer flows. This has been shown in the works of Sparrow and Cess (1995), Abdulhakeem and Sathiyanathan (2009), Magyari and Pantokratoras (2011).
In the present article, a detailed attempt is made to investigate an unsteady, magnetohydrodynamic flow, heat and mass transfer of non-Newtonian viscoelastic second grade past an infinite vertical porous plate in the presence of nonlinear thermal radiation in an optically thick media, thermal diffusion and diffusion thermo effects. The present analysis focuses on the nonlinearized form of radiative heat flux which depicts the real heat emission or conduction in the energy characteristics combined with Soret and Dufour effects for mixed convective transport of second grade fluid. The problem has not been previously considered to the best of the authors' knowledge. Moreover, the present investigation of MHD flow, heat and mass transfer of a second grade fluid becomes the basis of some engineering applications.

2. Mathematical Formulation

Consider a transient mixed convective magnetohydrodynamic flow, heat and mass transfer of an incompressible second grade fluid. The fluid is presumed to pass through an infinite vertical porous plate in the presence of nonlinearized thermal radiation, diffusion thermo and thermal diffusion effects. Choosing the x'- axis along the plate vertically upwards, y'- axis is normal to the plate. The porous plate moved in its plane with an initial velocity $U(t)$. The surface temperature and species concentration of the plate are respectively T_w and C_w while the respective free stream temperature and species concentration are $T_\infty$and C_∞ which are infinitesimally small. The plate is assumed to be infinitely long such that the physical variables are only functions of $y'$and t'. The conducting fluid is permeated by an imposed uniform magnetic field $B = (0, B_0, 0)$ which acts transversely to the flow direction. Assuming the magnetic Reynolds number is sufficiently small so that the induced magnetic field can be neglected, the magnetic force is $J \times B$. Under these assumptions, the Lorentz force becomes $\sigma (V \times B) \times B = -\sigma B_0^2 V$ where σ is the electrical conductivity, J is the current density and V is the velocity vector. All other thermo-physical and chemical properties are presumed to be constant. Thus, the continuity equation for the velocity field becomes:

$$u' = u'\left(y', t'\right), v' = -V_0 \tag{1}$$

where u' and v' are the velocities of the fluid along x' and y' axes respectively, and $V_0 > 0$ corresponds to suction velocity.

2.1 Flow Analysis

Following Asghar *et. al.* (2009), the constitutive relation of a homogeneous incompressible fluid of second grade is of the form:

$$\tau = -p\,I + \mu\,A_1 + \alpha_1\,A_2 + \alpha_2\,A_1^2 \tag{2}$$

where τ refers to the Cauchy stress tensor, μ is the dynamic viscosity, $-pI$ represents the spherical stress due to the constraint of incompressibility A_1 and A_2 are the first two Rivlin-Erickson tensors. According to Rivlin and Ericksen (1955) and Dunn and Rajagopal (1995) for a thermodynamically compatible second grade fluid, the material moduli satisfy the following restriction: $\mu \geq 0$, $\alpha_1 \geq 0$, $\alpha_1 + \alpha_2 = 0$ and A_1 and A_2 are defined by: $A_1 = grade\,V + (grade\,V)^{T^*}$ and $A_2 = \frac{dA_1}{dt} + A_1\,(grade\,V) + (grade\,V)^{T^*}\,A_1$
where T^* signifies the matrix transpose and t is the time.
A detailed thermodynamic, stability and boundedness analysis of the second grade fluid model has been given by Dunn and Fosdick (1974) and Dunn and Rajagopal (1995).
Hence, the stress components (2) by virtue of (1) are:

$$\tau_{x'x'} = -p + \alpha_2 \left(\frac{\partial u'}{\partial y'}\right)^2 \tag{3}$$

$$\tau_{y'y'} = -p + (2\alpha_1 + \alpha_2) \left(\frac{\partial u'}{\partial y'}\right)^2 \tag{4}$$

$$\tau_{z'z'} = -p \tag{5}$$

$$\tau_{x'y'} = \mu \frac{\partial u'}{\partial y'} - \alpha_1 V_0 \frac{\partial^2 u'}{\partial y'^2} + \alpha_1 \frac{\partial^2 u'}{\partial y' \partial t} \tag{6}$$

$$\tau_{x'z'} = \tau_{z'y'} = 0 \tag{7}$$

where $\tau_{x'y'} = \tau_{y'x'}$, $\tau_{x'z'} = \tau_{z'x'}$, $\tau_{y'z'} = \tau_{z'y'}$.
Using the stress components and the velocity field in the basic conservation of momentum equation:

$$\rho \frac{DV_i}{Dt} = -\tau'_{,i} + \rho X_i + \tau'_{ij,j} \tag{8}$$

where $\frac{D}{Dt}$ is the material derivative and X_i represents the external force per unit mass in i^{th}direction. The body force ρX_i in terms of magnetic field and gravitational force and surface forces τ in terms of normal and shear stresses are considered in equation (8). Using the similarity transforms for scaling respective heat transport and species concentration equations for heat and mass transfer analysis; $\theta = \frac{T'-T'_\infty}{T'_w-T'_\infty}$ and $\phi = \frac{C'-C'_\infty}{C'_w-C'_\infty}$ where θ and ϕ are dimensionless temperature and species concentration respectively, the equation of motion gives:

$$\begin{aligned}\frac{\partial u'}{\partial t'} &= V_0\frac{\partial u'}{\partial y'} + \frac{\mu}{\rho}\frac{\partial^2 u'}{\partial y'^2} + \frac{\alpha_1}{\rho}\left(\frac{\partial^3 u'}{\partial y'^2 \partial t'}\right) - \frac{\alpha_1 V_0}{\rho}\frac{\partial^3 u'}{\partial y'^3} \\ &+ g'\beta_T\left(T'_w - T_\infty\right)\theta + g'\beta_c\left(C'_w - C'_\infty\right)\phi\end{aligned} \tag{9}$$

2.2 Heat transfer analysis

The conservation of energy equation for the problem over the porous plate, neglecting viscous dissipation, Joule heating and work done to deformation, in the presence of diffusion thermo thermal diffusion effects is obtained as:

$$\frac{DT'}{Dt'} = \frac{\kappa}{\rho C_p}\frac{\partial^2 T'}{\partial y'} - \frac{1}{\rho C_p}\frac{\partial q_r}{\partial y'} + \frac{D_m K_T}{C_s C_p}\frac{\partial^2 C'}{\partial y'^2} \tag{10}$$

where ρ is the density, C_p is the specific heat at constant pressure, K is the thermal conductivity, q_r is the radiative heat flux, D_m is the mass diffusivity, C_s is the concentration susceptivity and K_T is the thermal diffusion ratio.

Adopting the radiative heat flux for optically thick media with a nonlinearized Rosseland approximation as proposed by Sparrow and Cess (1995), Magyari and Panntokratoras (2011) and Abdulhakeem and Sathiyanathan (2009) as:

$$q_r = \frac{\partial}{\partial y'}\left(\frac{-4\sigma^*}{3\xi}\frac{\partial T^4}{\partial y'}\right) \tag{11}$$

where σ^* is the Stefan-Boltzmonn constant and ξ represents the mean absorption coefficient.

Hence, the energy equation (10) for the temperature field using equations (1) and (11) becomes:

$$\frac{\partial T'}{\partial t'} - V_0\frac{\partial T'}{\partial y'} = \frac{k}{\rho C_p}\frac{\partial^2 T'}{\partial y'^2} + \frac{\partial}{\partial y'}\left(\frac{-4\sigma^*}{3\xi}\frac{\partial T^4}{\partial y'}\right) + \frac{D_m K_T}{C_s C_p}\frac{\partial^2 C'}{\partial y'^2} \tag{12}$$

2.3 Mass Transfer Analysis

The conservation of species concentration equation for the second grade fluid with chemical reaction over the surface of the vertical porous plate is:

$$\frac{DC'}{Dt} = D_m\frac{\partial^2 C'}{\partial y'^2} + \frac{D_m K_T}{T_m}\frac{\partial^2 T'}{\partial y'^2} \tag{13}$$

where T_m is the mean fluid temperature.

Employing equation (1), the species concentration equation becomes:

$$\frac{DC'}{Dt} = V_0\frac{\partial C'}{\partial y'} + D_m\frac{\partial^2 C'}{\partial y'^2} + \frac{D_m K_T}{T_m}\frac{\partial^2 T'}{\partial y'^2} \tag{14}$$

The initial and boundary conditions are:

$$t' \leq 0 : y' = 0, u' = 0, T' = 0, C' = 0 \tag{15}$$

$$t' > 0 : u'\left(0, t'\right) = U\left(t\right) = \frac{U^{2n+1}}{V^{n}} \ell^{a't'} t'^{n} \ when \ y' = 0 \tag{16}$$

$$T'\left(0, t'\right) = \left(T'_{w} - T'_{\infty}\right) + T'_{\infty} = 1, C'\left(0, t'\right) = \left(C'_{w} - C'_{\infty}\right) + C'_{\infty} = 1 \ when \ y' = 0 \tag{17}$$

$$u'\left(\infty, t'\right) = 0, \frac{\partial u'\left(\infty, t\right)}{\partial y'} = 0 \ as \ y' \to \infty \tag{18}$$

$$T'\left(\infty, t'\right) \to T'_{\infty} = 0, C'\left(\infty, t'\right) \to C'_{\infty} = 0 \ as \ y' \to \infty \tag{19}$$

The following dimensionless variables are introduced:

$$u = \frac{u'}{U}, y = \frac{y'U}{\upsilon}, a = \frac{a'\upsilon}{U^{2}}, t = \frac{t'U^{2}}{\upsilon} \tag{20}$$

Then, equations (9), (12) and (14) become:

$$\frac{\partial u}{\partial t} = \alpha \frac{\partial^{3} u}{\partial y^{2} \partial t} - S\alpha \frac{\partial^{3} u}{\partial y^{3}} + \frac{\partial^{2} u}{\partial y^{2}} + S\frac{\partial u}{\partial y} - Mn\, u + \lambda\left(\theta + N\phi\right) \text{‘} \tag{21}$$

$$\frac{\partial \theta}{\partial t} = \frac{1}{\Pr}\left[1 + \frac{4Rt}{3}\left(\theta + Cr\right)^{3}\right]\frac{\partial^{2}\theta}{\partial y^{2}} + \frac{4Rt}{\Pr}\left(\theta + Cr\right)^{2}\left(\frac{\partial \theta}{\partial y}\right)^{2} + Du\frac{\partial^{2}\phi}{\partial y^{2}} + S\frac{\partial \theta}{\partial y} \tag{22}$$

$$\frac{\partial \phi}{\partial t} = \frac{1}{\Pr Le}\frac{\partial^{2}\phi}{\partial y^{2}} + Sr\frac{\partial^{2}\theta}{\partial y^{2}} + S\frac{\partial \phi}{\partial y} \tag{23}$$

where $S = \frac{V_0}{U}$, $\alpha = \frac{\alpha_1 U^2}{\rho \upsilon^2}$, $\Pr = \frac{\mu\, Cp}{\kappa}$, $Le = \frac{\alpha_d}{D_m}$, $Rt = \frac{4\sigma^*(T'_w - T'_\infty)}{\xi\,\kappa}$,

$$Cr = \frac{T'_{w}}{\left(T'_{w} - T'_{\infty}\right)}, Du = \frac{D_m K_T \upsilon\ \left(C'_{w} - C'_{\infty}\right)}{C_s C_p U^{2}\left(T'_{w} - T'_{\infty}\right)}, Sr = \frac{D_m K_T \upsilon\left(T'_{w} - T'_{\infty}\right)}{T_m U^{2}\ \left(C'_{w} - C'_{\infty}\right)},$$

$$\alpha_d = \frac{\kappa}{\rho C_p}, Re = \frac{u'^{2}}{\upsilon^{2}}, \lambda = \frac{Gr_T u'^{2}}{Re^{2}}, N = \frac{\beta_C\ \left(C'_{w} - C'_{\infty}\right)}{\beta_T\left(T'_{w} - T'_{\infty}\right)}$$

are suction parameter, second grade parameter, Prandtl number, Lewis number, thermal radiation parameter, temperature difference parameter, Dufour number, Soret number, thermal diffusivity, Reynolds number, mixed convection parameter and concentration buoyancy parameter respectively.

The initial and mixed boundary conditions (15) - (19) are also non-dimensionalized using (20) to obtain the following initial and boundary conditions:

$$t \le 0 : y = 0, \quad u = 0, \quad \theta = 0, \quad \phi = 0; \tag{24}$$

$$t > 0 : u = e^{a\,t} t^{n}, \theta = 1, \phi = 1 \ when \ \ y = 0; \tag{25}$$

$$u \to 0, \frac{\partial u}{\partial y} \to 0, \theta \to 0, \phi \to 0 \; as \;\; y \to \infty \tag{26}$$

3. Method of Solution

The governing coupled nonlinear time-based partial differential equations (21) - (23) alongside the initial and mixed boundary conditions (25) - (26) are solved by employing an implicit finite difference numerical scheme of Crank-Nicolson approach as expatiated by Conte and De Boor (1980), Jain *et. al.* (1977) and Kreyzig (2004). Based on the transient state conditions, the governing equations (21) - (23) are discretized. The convergent term r used in the discretization process does not restrict the value of r to be chosen for the emerging parameters involved. The implicit finite difference equations corresponding to the governing partial differential equations are as follows:

(27)

$$\begin{aligned} u_{i,j+1} &= \left(\tfrac{r\,h\,S}{4} + \tfrac{r}{2} + \tfrac{\alpha}{h^2} - \tfrac{\alpha\,r\,S}{h}\right) u_{i+1,j+1} + \left(\tfrac{r}{2} - \tfrac{r\,h\,S}{4} + \tfrac{\alpha}{h^2} - \tfrac{\alpha\,r\,S}{h}\right) u_{i-1,j+1} \\ &+ \left(\tfrac{rhS}{4} + \tfrac{r}{2}\right) u_{i+1,j} + \left(\tfrac{r}{2} - \tfrac{r\,h\,S}{4} + \tfrac{\alpha}{h^2}\right) u_{i-1,j} - 2\,\left(\tfrac{r}{2} + \tfrac{\alpha}{h^2}\right) u_{i+1,j} - 2\,\left(\tfrac{r}{2} + \tfrac{\alpha}{h^2}\right) u_{i,j} \\ &+ \tfrac{\alpha}{h^2} u_{i+1,j} - \tfrac{\alpha\,r\,S}{2h} \left[\left(-u_{i-2,j+1} + u_{i+2,j+1}\right) - \left(-u_{i-2,j} + 2u_{i-1,j} - 2u_{i+1,j} + u_{i+2,j}\right)\right] \\ &+ 2rh^3\lambda\,\left(\theta_{i,j+1} + \theta_{i,j} + N\left(\phi_{i,j+1} + \phi_{i,j}\right)\right) - u_{i,j} \end{aligned}$$

(28)

$$\begin{aligned} \theta_{i,j+1} &= \tfrac{r}{\Pr}\left[1 + \tfrac{4Rt}{3}\left(\theta^3_{i,j} + 3\theta^2_{i,j} Cr + 3\theta_{i,j} Cr^2 + Cr^3\right)\right] \begin{pmatrix} \theta^2_{i,j+1} - 2\,\theta_{i,j+1} \\ \theta_{i-1,j+1} + 2\,\theta^2_{i-1,j+1} \end{pmatrix} \\ &\tfrac{rRt}{\Pr}\left(\theta^2_{i,j} + 2\,Cr\theta_{i,j} + Cr^2\right)\left(\theta^2_{i,j+1} - 2\theta_{i,j+1}\theta_{i-1,j+1} + \theta^2_{i-1,j+1}\right) \\ &+ rDu\left(\theta_{i+1,j+1} - 2\theta_{i,j+1} + \theta_{i-1,j+1}\right) + \tfrac{rh\,S}{2}\left(\theta_{i,j+1} - \theta_{i-1,j+1}\right) + \theta_{i,j} \end{aligned}$$

$$\begin{aligned} \phi_{i,j+1} &= \tfrac{r}{\Pr Le}\left(\phi_{i+1,j+1} - 2\phi_{i,j+1} + \phi_{i-1,j+1}\right) \\ &+ r\,Sr\left(\phi_{i+1,j+1} - 2\phi_{i,j+1} + \phi_{i-1,j+1}\right) + \tfrac{r\,h\,S}{2}\left(\phi_{i+1,j+1} - \phi_{i-1,j+1}\right) + \phi_{i,j} \end{aligned} \tag{29}$$

where i designates the grip point along y-direction, j along t-direction and $r = {\Delta t}/{h^2}$.

With the finite difference equations (27) - (29), the equations of motion, energy and species concentration are reduced to system of nonlinear algebraic equation. The step-size $h = 0.05$ with the step $t = 0.1$ are utilized in all cases for the discretization of the governing equations and the values of $u(y,t)$,$\theta\,(y,t)$ and $\phi\,(y,t)$ are known at all grid point from the initial conditions when $t = 0$. Hence, modified Newton's iterative technique is therefore employed to solve the system of nonlinear equations. After the computing values corresponding to each i at a time level, the computations are executed by moving along $y-$direction and the values at the next time level are determined in the same manner for the numerical solutions.

It should be noted that the implicit nature of Crank-Nicolson technique of finite difference method is unconditionally stable and has a local truncation error of

$O\left[(\Delta t)^2, h^2\right]$ which tends to zero as Δt and h^2 tend to zero. Also, the method gives stable solutions and there is no drawback of conditional stability from one level of iteration to the next. The difference equations corresponding to the governing equations do not automatically guarantee the convergence of the mesh $h \to 0$, but maximum numerical efficiency is achieved with the tridiagonal procedure for establishing solutions of two point conditions for equation (28) and (29), and three point conditions for equation (27). The above procedure is transformed into MAPLE code as described by Heck (2003). The convergence of the entire process was satisfactory and the numerical stability (consistency) of the method was generated by the implicit nature of the finite difference scheme.

4. Discussion of Results

The effects nonlinearized thermal radiation, thermal diffusion and diffusion thermo on transient mixed convective magnetohydrodynamic flow, heat and mass transfer of an incompressible viscoelastic second grade fluid past a vertical porous plate is investigated. The research exhibits velocity distributions when a vertically upward plate suddenly sets in motion at a velocity $U(t)$ in its own plane for $n = 0.3$ which corresponds to a variable acceleration at any point within the fluid with considerations for temperature and species concentration distributions. The governing equations of the flow field are solved by employing an efficient Crank-Nicolson finite difference technique with modified Newton's iterative technique and approximate solutions are obtained for velocity, temperature and species concentration distributions. The influences of some controlling parameters on the flow field are analyzed and discussed with the aid of velocity profiles (Figures 1-8), temperature profiles (Figures 9-13) and species concentration profiles (Figures 14-17).

4.1 Velocity Profiles

During numerical calculations, the values of the some parameters have been realistically chosen while the values of other parameters are chosen arbitrarily. The effect of the suction parameter on the transient velocity distributions are shown in Figure 1. It is observed from Figure 1 that the fluid velocity decreases with the increase in suction parameter S for the variable acceleration at any point within the fluid. This implies that suction which is the removal of fluid from the domain via the porous plate can be used to control the fluid dynamics. Thus, suction enhances adherence of the fluid to the plate which in turn retards the flow. Figure 2 displays the influence of the viscoelastic second grade parameter α on the velocity distribution. It is clear from Figure 2 that the fluid velocity increases for the variable acceleration when the second grade parameter α increases. This implies that an increase in the fluid velocity corresponds to a reduction of the velocity boundary layer thickness. This observation, on the behaviour of hydromagnetic viscoelastic second grade flow, agrees with that reported by Hayat *et. al.* (2008).

Figure 3 analyzed the effect of magnetic interaction parameter Mn on the velocity distribution for variable accelerations along the vertical porous plate. It is obvious from Figure 3 that an increase in Mn leads to a reduction in the fluid velocity at any point within the fluid. The implication of this is that the presence of transverse magnetic field sets in Lorentz force which results in a retarding force on the velocity field. Therefore, as the magnetic interaction parameter increases, so does the retarding force on the velocity field and hence, there is a significant reduction in the velocity of the fluid flow. Figures 4 and 5 reveal that the dimensionless concentration buoyancy N and mixed convection λ parameters have the same effects on the velocity distribution. They both enhance the velocity profiles thereby decreasing the momentum boundary layer thicknesses. Similarly, Figures 6 and 7 express the variations velocity profiles with Prandtl Prand Lewis Le numbers respectively. They are found to be decreasing functions of the velocity distributions. The effect of Soret number on the velocity profile is displayed in Figure 8. The velocity profile is found to increase with an increase in the values of Sr.

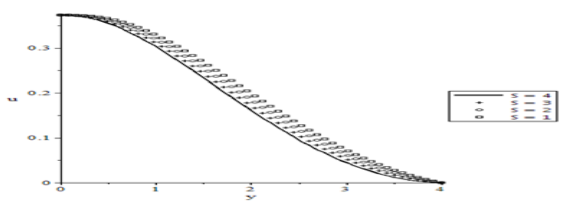

Figure 1: Velocity profile for S when $\alpha = 3$, $Mn = 0.5$, $\lambda = 10$ and $N = 10$

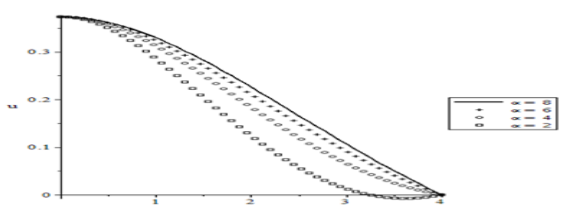

Figure 2: Velocity profile for α when $S = 4$, $Mn = 0.5$, $\lambda = 10$ and $N = 10$

4.2 Temperature Profiles

Figures 9-13 illustrate the influences of pertinent parameters in the flow field on the dimensionless temperature profiles. Figure 9 displays the variation of suction parameter S on the velocity profile. The thermal boundary layer thickness is reduced by the increasing values of S while other flow parameters are kept constant. This is anticipated as there is a reduction in velocity of the fluid as a result of an increment in the values of S in the flow regime, thereby reducing the

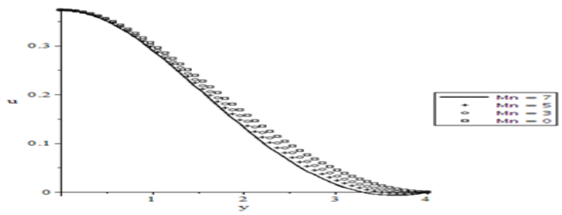

Figure 3: Velocity profile for Mn when $\alpha = 3$, $S = 4$, $\lambda = 10$ and $N = 10$

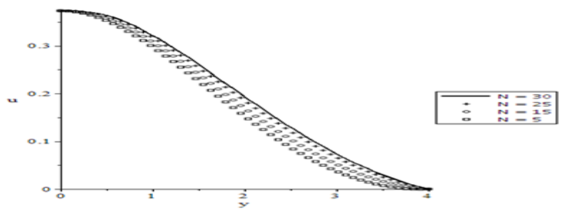

Figure 4: Velocity profile for N when $\alpha = 3$, $Mn = 0.5$, $\lambda = 10$ and $S = 4$.

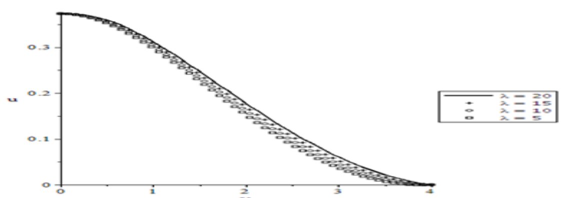

Figure 5: Velocity profile for λ when $\alpha = 3$, $Mn = 0.5$, $S = 10$ and $N = 10$.

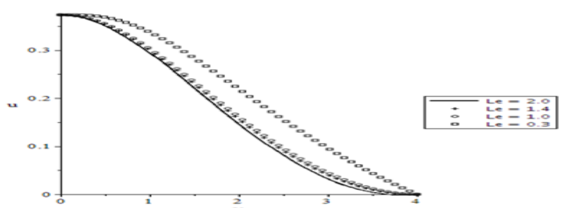

Figure 6: Velocity profile for Le when $\alpha = 3$, $Mn = 0.5$, $\lambda = 10$ and $N = 10$.

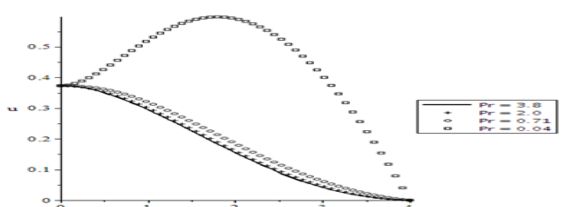

Figure 7: Velocity profile for Pr when $\alpha = 3$, $Mn = 0.5$, $\lambda = 10$ and $N = 10$

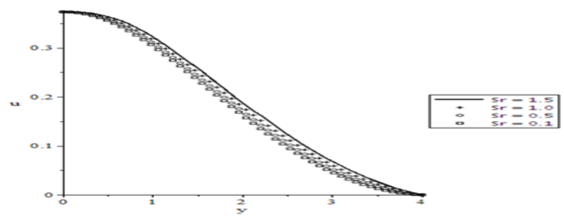

Figure 8: Velocity profile for Sr when $\alpha = 3$, $Mn = 0.5$, $\lambda = 10$ and $N = 10$

temperature of the flow region. The effect of the thermal radiation parameter Rt on the temperature profile is illustrated in Figure 10. As the values of Rt increases, it also increases the temperature profile. Thus, the thermal radiation parameter is found to enhance the thermal boundary layer thickness in the flow regime. Figure 11 has been portrayed to show the effects of Dufour number on the temperature distribution. The thermal boundary layer thickness is found to be enhanced with increasing values of Du. Figure 12 depicts the influence of temperature difference Cr on the temperature distribution across the thermal boundary layer. The consequence of increasing the values of Cr increases the fluid temperature thereby reducing the thickness of the thermal boundary layer formed away from the surface. Figure 13 presents the effect of Prandtl number Pr on the temperature profile. It is found that an increase in the value of Prreduces the thermal boundary layer thickness. Higher estimation of Pr is found to decay the temperature field. This is due to the fact that Prexpresses the ratio of thermal diffusivity to momentum diffusivity. Thus, small values of Pr implies that the thermal diffusivity dominates and for higher estimation of Pr, the momentum diffusivity dominates.

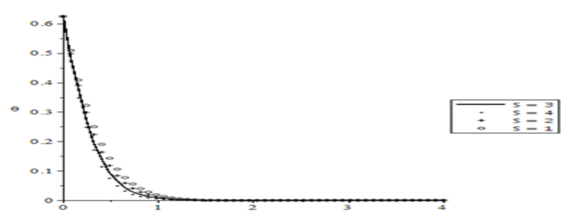

Figure 9: Temperature profile for S when $\Pr = 0.71$, $Le = 1$, $Rt = 0.5$ and $Du = 0.3$

4.3 Species Concentration Profiles

The species concentration of the flow field suffers a substantial change with the variation of the flow parameters such as the suction parameter S, Prandtl number Pr, Lewis number Le and Soret parameter Sr. It is observed from Figure 14 that when there is an increase in the values of suction parameter, there is a reduction in the species concentration field. Figure 15 describes the effects of Soret number

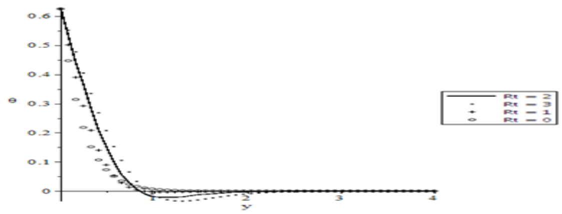

Figure 10: Temperature profile for Rt when $\Pr = 0.71$, $Le = 1$, $Cr = 0.5$ and $Du = 0.3$

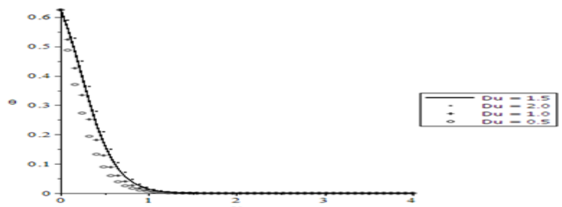

Figure 11: Temperature profile for Du when $\Pr = 0.71$, $Le = 1$, $Rt = 0.5$ and $Cr = 0.5$

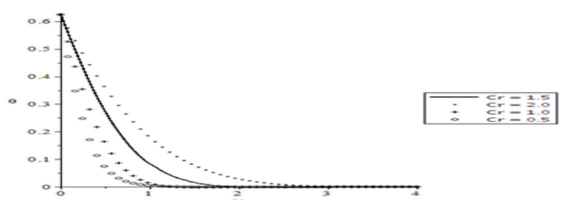

Figure 12: Temperature profile for Cr when $\Pr = 0.71$, $Le = 1$, $Rt = 0.5$ and $Du = 0.3$

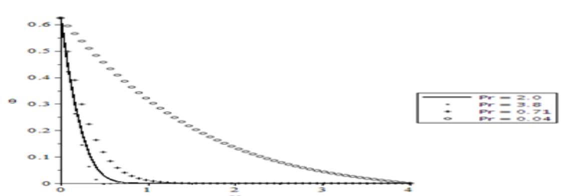

Figure 13: Temperature profile for Pr when $Cr = 0.5$, $Le = 1$, $Rt = 0.5$ and $Du = 0.3$

Sr on the species concentration field. The Soret effect is a mass flux due to a temperature gradient and the Dufour effect is enthalpy flux due to a concentration gradient and appears in the energy equation. It is clear that Sr decreases the species concentration field, thereby decreasing the species concentration boundary thickness in the flow regime. Figure 16 captures the influence of Lewis number on the species concentration distribution. It is observed that for an increasing values of Le, the species concentration becomes decreased. This also implies a reduction in the species concentration boundary layer thickness. The variation of ϕ with different values of Pr is indicated by Figure 17. It is clear that the Prandtl number decreases the species concentration field and the consequential effect is noticed in the species boundary layer thickness. This influence of Pr on the species concentration profile is the same as its effects on temperature profile.

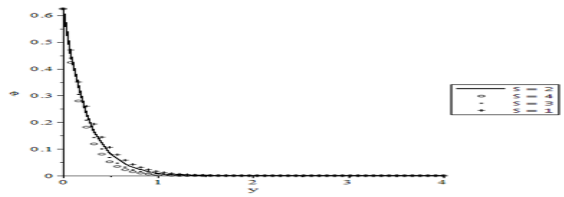

Figure 14: Species concentration profile for S when $\Pr = 0.71$, $Le = 1$ and $Sr = 0.5$

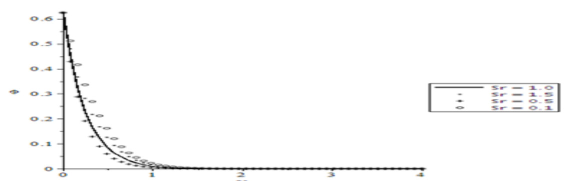

Figure 15: Species concentration profile for Sr when $\Pr = 0.71$, $Le = 1$, $S = 4$ and $\alpha = 3$

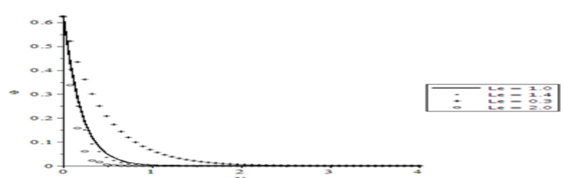

Figure 16: Concentration profile for Sr when $\Pr = 0.71$, $Le = 1$, $S = 4$ and $\alpha = 3$

CONCLUSIONS

In the present investigation, the transient mixed convective flow, heat and mass transfer of a viscoelastic second grade fluid past a vertical porous plate in the presence of nonlinearized thermal radiation, thermal diffusion and diffusion thermo effects is studied. The governing time-based partial differential equations with initial and mixed boundary conditions are solved using an efficient numerical scheme of implicit Crank-Nicolson finite difference technique with the modified

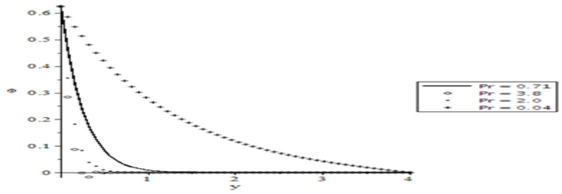

Figure 17: Species concentration profile for Sr when $\Pr = 0.71$, $Le = 1$, $S = 4$ and $\alpha = 3$

Newton's iterative method. Simulation of the scheme is done with the aid of MAPLE codes to obtain approximate solutions of the problem. The solution procedure is valid for all values of emerging viscoelastic second grade parameters. The conclusions of the study are as follows:

(1) The velocity increases significantly with increasing values of viscoelastic second grade, mixed convection, concentration buoyancy parameters and Soret number;
(2) Increasing values of suction, concentration buoyancy and magnetic interaction parameters as well as Soret number increase the momentum boundary layer thicknesses;
(3) The fluid temperature increases as the values of thermal radiation parameter, temperature difference parameter and Dufour number increase while suction parameter and Prandtl number decrease the thermal boundary layer thicknesses;
(4) The species concentration of the fluid decreases with increasing values of suction parameter, Soret, Lewis and Prandtl numbers.

References

[1] Abdul-Hakeem A. K. and Sathiyanathan K. (2009). An analytic solution of an oscillatory flow through a porous medium with radiation effect. Nonlinear Analysis: Hybrid System; **3**: 288-295.

[2] Abel M. S., Prasad K. V. and Mahaboob A. (2005). Buoyancy force and thermal radiation effect in MHD boundary layer viscoelastic fluid flow over continuously moving stretching surface. Int. J. Therm. Sci.; **44**: 465-476.

[3] Afify A. A. (2009). Similarity solution in MHD effects of thermal diffusion and diffusion thermo on free convective heat and mass transfer over stretching surface considering suction or injection. Communications in Nonlinear Science and Numerical Simulation; **14** (5): 2202-2214.

[4] Ali M. and Awais M. (2014). Laplace transform method for unsteady thin film flow of a second grade fluid through a porous medium. Journal of Modern Physics; **05** (03): 103-106. doi: 10.4236/jmp.2014.53017.

[5] Ariel O. D. (2002). On exact solution of flow problems of a second grade fluid through two parallel plates. Int. J. Eng. Sci.; **40**: 913-941.

[6] Asghar S., Hanif K., Hayat T. and Khalique C. M. (2007). MHD non-Newtonian flow due to non-coaxial rotations of an accelerated disk and fluid at infinity. Comm. Nonlinear Sci. Numer. Simul.; **12**: 465-485.

[7] Asghar S., Hayat T. and Ariel P. D. (2009). Unsteady Couette flows in second grade fluid with variable material properties. Commun. Non-linear Sci. Numer. Simul.; **14**: 54-159.

[8] Baoku I. G., Israel-Cookey C. and Olajuwon B. I. (2012). Influence of thermal radiation on a transient MHD Couette flow through a porous medium. Journal of Applied Fluid Mechanics; **5**: 81-87.

[9] Baoku I. G., Onifade Y. S., Adebayo L. O. and Yusuff K. M. (2015). Heat and mass transfer in a second grade fluid over a stretching vertical surface in a porous medium. International Journal of Applied Mechanics and Engineering; **20** (2): 239-255.

[10] Bandelli R. and Rajagopal K. R. (1995). Startup Flows of Second Grade Fluids in domains with one dimension. Int. J. Non-Linear Mech.; **30**: 517-539.

[11] Bhattacharyya S., Pal A. and Gupta A. S. (1998). Heat transfer in the flow of a visco-elastic fluid over a stretching surface. Heat Mass Transfer; **34**: 1851-1856.

[12] Chen C. I., Chen C. K. and Yang Y. T. (2003). Unsteady unidirectional flow of a second grade fluid between the parallel plates with different given volume flow rate conditions. Appl. Maths. Comput.; **137** (2): 437-450.

[13] Conte S. D. and De Boor C. (1980). Elementary Numerical Analysis: An Algorithmic Approach, McGraw-Hill Inc., New York.

[14] Cortell B. (2007). Viscoelastic fluid flow and heat transfer over a stretching sheet under the effect under the effects of non-uniform heat source, viscous dissipation and thermal radiation. Int. J. Heat Mass Transfer; **50**: 3152-3162.

[15] Cortell R. (2006). Flow and heat transfer of an electricity conducting of second grade over stretching sheet to suction and a transverse magnetic field. Int. J. Heat Mass Transfer; **49**: 1851-1856.

[16] Dandapat B. S. and Gupta A. S. (1989). Flow and heat transfer in a visco-elastic fluid over a stretching sheet. Int. J. Non-Linear Mech.; **24**: 215-219.

[17] Dunn J. E. and Fosdick R. L. (1974). Thermodynamics, stability and boundedness of fluid of complexity and fluids of second grade. Archive for Rational Mechanics and Analysis; **56** (3): 191-252.

[18] Dunn J. E. and Rajagopal K. R. (1995). Fluids of differential type: critical review and thermodynamic analysis. Int. J. Eng. Sci.; **33**: 689-729.

[19] Eckert E. R. and Drake R. M. (1972). Analysis of Heat and Mass Transfer. New York: McGraw Hill.

[20] Jain M. K., Iyengar S. R. K. and Saldanha J. S. V. (1977). Numerical Solution of a Fourth-order Ordinary Differential equations. Journal of Engineering Mathematics; **11** (4), 373-380.

[21] Hamad M. A. A., Uddin M. J. and Ismail A. I. M. (2012). Investigation of combined heat and mass transfer by Lie group analysis with variable diffusivity taking into account hydrodynamic slip and thermal convective boundary conditions. International Journal of Heat And Mass Transfer; **55** (4): 1355-1362.

[22] Hayat T., Abbas Z. and Sajid M. (2008). Heat and mass transfer analysis on the flow of a second grade fluid in presence of chemical reaction. Phys. Lett. A.; **372**: 2400-2408.

[23] Hayat T., Fetecau C. and Sajid M. (2008). Analytic solution for MHD transient rotating flow of a second grade fluid in a porous space. Nonlinear Analysis: Real World Applications; **9**: 1619-1627.

[24] Heck A. (2003). Introduction to Maple, 3^{rd} Edition, Springer-Verlag, Germany.

[25] Khan A., Abro A. K., Tassaddiq A. and Khan I. (2017). Atangana-Baleanu and Caputo Fabrizio analysis of fractional derivative for heat and mass transfer of second grade fluids over a vertical plate. Entropy; **19**: 279. doi: 10.33910/e19080279.

[26] Kreyzig E. (2004). Advanced Engineering Mathematics, 8^{th} Edition, John Wiley and Sons, Inc., New York.

[27] Magyari E. and Pantokratoras A. (2011). Effect of thermal radiation in the linearized Rosseland approximation on the heat transfer characteristics of various boundary layer flows. International Communication in Heat and Mass Transfer; **38**: 554-556.

[28] Makinde O. D. and Mhone P. Y. (2005). Heat transfer to MHD oscillatory flow in a channel filled with porous medium. Romanian J. Phys.; **50**: 931-938.

[29] Makinde O. D. (2005). Free-convection flow with thermal radiation and mass transfer past a moving porous plate. Int. Comm. Heat Mass Transfer; **32**: 1411-1419.

[30] Massoudi M. and Maneschy C. E. (2004). Numerical solution to the flow of a second grade fluid over a stretching sheet using the method of quasi-linearization. Appl. Math. Comput.; **149**: 165-173.

[31] Nabil T. M., El-Dabe, Rafaie Ali. A., El-Shekhiphy A. A. and Shalaby G. A. (2017). Non-linear heat and mass transfer of second grade fluid flow with hall currents and thermophoresis effect. Applied Mathematics and Information Science; **11** (1): 267-280.

[32] Nataraja H. R., Sharma M. S. and Naggeshwar Rao B. (1998). Non-similar solution for Flow and heat transfer in a viscoelastic fluid over a stretching sheet. Int. J. Non-Linear Mech.; **33**: 357-361.

[33] Olajuwon B. I. and Baoku I. G. (2014). Numerical study of heat and mass transfer in a transient third grade fluid flow in the presence of heat source, chemical reaction and thermal radiation. Daffodil International University Journal of Science and Technology; **9** (2): 25-36.

[34] Olanrewaju P. I. (2010). Effects of a transient free convective flow with radiative heat transfer past a flat plate moving through a binary mixture. Pacific Journal of Science and Technology; **11** (1): 673-685.

[35] Popoola A. A., Baoku I. G. and Olajuwon B. I. (2016). Heat and mass transfer on MHD viscoelastic fluid flow in the presence of thermal diffusion and chemical reaction. Journal of Heat and Technology; **34**: 15-26.

[36] Prasad K. V., Subhas A. and Joshi A. (2000). Oscillatory motion of a visco-elastic fluid over a stretching sheet in a porous media. Journal of Porous Media; **3** (1): 61-68.

[37] Prasad K. V., Subhas A. and Khan S. K. (2001). Momentum and heat transfer in visco-elastic fluid flow in porous medium over a non-isothermal stretching sheet, Int. J. Num.Methods Heat Fluid Flow; **10** (8): 786-801.

[38] Rajagopal K. R., Na T. Y. and Gupta A. S. (1984). Flow of visco-elastic fluid over a stretching sheet. Rheol. Acta; **23**: 213-215.

[39] Raptis A. and Perdikis C. (1999). Radiational second free convection flow past moving plate, Appl. Mech. Eng.; **4** (4): 817-821.

[40] Raza N. (2017). Unsteady rotational flow of a second grade fluid with integer Caputo time fractional derivative. Punjab University Journal of Mathematics; **49** (3): 15-25.

[41] Rivlin R. S. and Ericksen J. L. (1955). Stress Deformation Relation for Isotropic Materials. J. Rat. Mech. Anas.; **4**: 323-425.

[42] Sajid M., Ahmad I., Hayat T. and Ayub M. (2009). Unsteady flow and heat transfer of a second grade fluid over a stretching sheet. Commun. Non-Linear Sci. Numb. Simul.; **14**: 96-108.

[43] Siddheshwar P. G. and Mahabaleshwar U. S. (2005). Effect of radiation and heat transfer on MHD flow of visco-elastic liquid and heat transfer over a stretching sheet. Int. J. Non-linear Mech.; **40**: 807-820.

[44] Soundalgekar V. M. (1974). Stoke's problem for elastico-viscous fluid. Rheol. Acta; **13**: 744-746.

[45] Subhas A. and Veena P. H. (1998). Visco-elastic fluid flow and heat transfer in porous medium over a stretching sheet. Int. J. Non-linear Mech.; **33**: 531-540.

[46] Sparrow E. M. and Cess R. D. (1995). Hemisphere publ. Stuart-J. T, In Proc. Roy. Soc. London; **A231**: 116.

[47] Vajravelu K. and Rollins D. (2004). Hydromagnetic flow of a second grade fluid over stretching sheet, Appl. Math. Comp.; **148**: 783-791.